A R T I C L E

Metadherin, a cell surface protein in breast tumors that mediates lung metastasis

Darren M. Brown and Erkki Ruoslahti*

Cancer Research Center, The Burnham Institute, 10901 North Torrey Pines Road, La Jolla, California 92037
*Correspondence: ruoslahti@burnham.org

Summary

We used a phage expression library of cDNAs from metastatic breast carcinoma to identify protein domains that bind to the vasculature of the lung, a frequent site of breast cancer metastasis. We found that one protein domain selectively targeted phage as well as cells to the lung. This domain is part of the protein metadherin, shown by gene expression profiling to be overexpressed in metastatic breast cancer. Immunostaining revealed that metadherin is overexpressed in breast cancer tissue and breast tumor xenografts. Antibodies reactive to the lung-homing domain of metadherin and siRNA-mediated knockdown of metadherin expression in breast cancer cells inhibited experimental lung metastasis, indicating that tumor cell metadherin mediates localization at the metastatic site.

Introduction

Tumor metastasis is a complex, multistep process in which cancer cells detach from the original tumor mass and establish metastatic foci at organ-specific sites (Fidler, 2001). The location of the metastatic site depends on the particular type of cancer and stage of disease. For example, breast cancer spreads first to the lungs and liver (Kamby et al., 1987; Rutgers et al., 1989; Tomin and Donegan, 1987). Later in the disease, breast cancer spreads to the central nervous system and bone (Amer, 1982; Boogerd, 1996). The metastatic phase of the disease is devastating, given that conventional treatments are usually ineffective and patients typically survive only a few years after diagnosis (Harris et al., 1997).

Several factors affect the location and growth of metastases. Depending on the bloodflow pattern from the primary tumor, certain tumor cells are carried preferentially to particular organs (Weiss, 1992). While in circulation, some tumor cells selectively recognize particular endothelial cell surface molecules that mediate cell adhesion to specific organs (Abdel-Ghany et al., 2001; Cheng et al., 1998; Johnson et al., 1993). The arrest of tumor cells at the metastatic site, be it through mechanical trapping in small capillaries or through adhesive interactions with the endothelium, is a necessary step for tumors to establish at a secondary site (Chambers et al., 2002; Orr and Wang, 2001). Once the tumor cells have seeded the target organ, the local microenvironment influences whether or not a particular cancer cell will proliferate (Fidler, 2001; Radinsky, 1995). Unfortunately, many of the factors that contribute to organ-specific metastasis have yet to be elucidated.

To identify tumor cell surface molecules that mediate breast cancer metastasis, we have used in vivo phage screening. This screening method has been used by our group to identify peptides and proteins that are capable of mediating selective in vivo localization of phage to individual organs as well as tumors and that reveal tissue-specific vascular differences (Arap et al., 1998, 2002; Laakkonen et al., 2002; Pasqualini and Ruoslahti, 1996; Porkka et al., 2002; Rajotte et al., 1998).

In this study, we isolated from phage expression libraries of breast carcinoma cDNAs a domain in a protein we call metadherin (for metastasis adhesion protein) that causes the phage to home specifically to lung microvasculature after intravenous injection. We show that the lung-homing domain of metadherin is extracellular. Antibodies to metadherin revealed high amounts of metadherin throughout human breast tumors and breast tumor xenografts while drastically lower levels of metadherin were present in normal breast tissue. We also show that antibodies reactive to the lung-homing domain of metadherin inhibited experimental breast cancer lung metastasis, as did siRNA-mediated knockdown of metadherin expression. These results suggest that metadherin plays an important role in breast cancer metastasis.

Results

Identification of cDNA clones by phage display
To identify candidate cell adhesion proteins that mediate breast cancer metastasis, we used an in vivo phage screening ap-

---

S I G N I F I C A N C E

Adhesive interactions with the endothelium have been shown to contribute to the localization and growth of tumors at particular secondary sites in experimental animals. In this report, we show that metadherin, a protein greatly overexpressed in breast cancers, mediates lung-specific dissemination of metastatic cells. Independent microarray data have identified high metadherin gene expression as a prognostic indicator of clinical metastasis in human breast cancer patients. Our results provide a possible mechanistic explanation for the clinical findings. Our demonstration that metastasis can be inhibited by blocking the lung-homing domain of metadherin with an antibody or by reducing metadherin expression identifies metadherin as a candidate target for therapeutic intervention in breast cancer and perhaps other cancers as well.
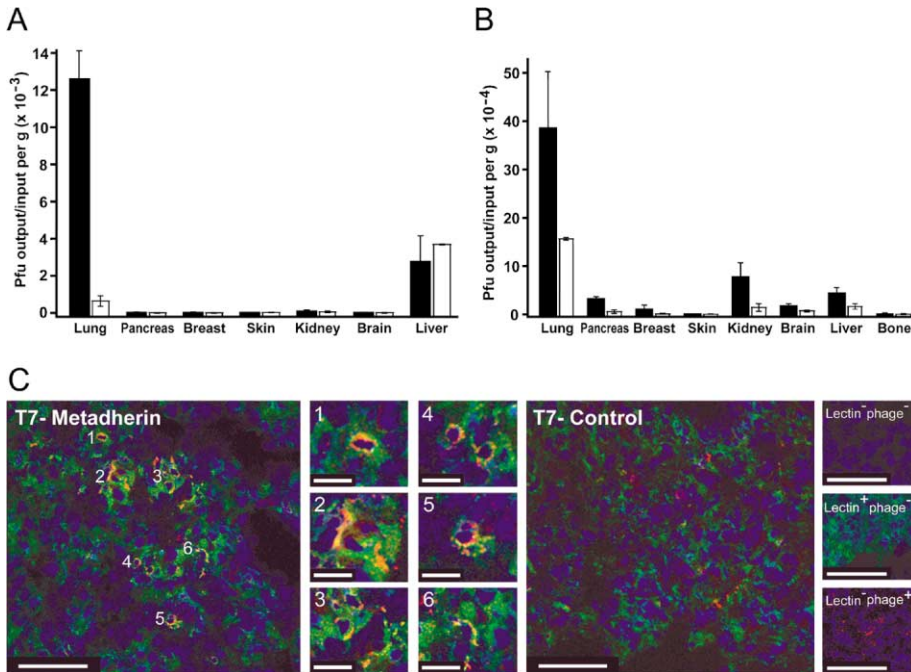
Figure 1. Homing specificity of metadherin phage

A: Metadherin (closed bars) and nonrecombinant (open bars) phage titers recovered from lung, pancreas, breast, skin, kidney, brain, and liver after injection into the tail vein of Balb/c mice and circulation for 5 min. Error bars represent mean ± SD for 2–7 experiments per variable.
B: Metadherin (closed bars) and nonrecombinant (open bars) phage titers recovered from lung, pancreas, breast, skin, kidney, brain, liver, and bone (tibia) after injection into the left ventricle of the heart of Balb/c mice and circulation for 5 min. Error bars represent mean ± SEM for 2–5 experiments per variable.
C: Confocal projections of anti-phage immunostained lungs from mice co-injected with fluorescein-labeled tomato lectin (green) and either metadherin phage (T7-metadherin) or T7-415 nonrecombinant phage (T7-Control). Control lungs were from noninjected mice (lectin⁻phage⁻), mice injected with lectin alone (lectin⁺phage⁻), or mice injected only with metadherin phage (lectin⁻phage⁺). Anti-phage antibody was detected with Alexa 594 goat anti-rabbit IgG antibody (red). Nuclei were stained with DAPI (blue). The scale bars correspond to 50 μm, except in panels 1–6, where the scale bars correspond to 10 μm.

proach. We selected the highly metastatic, Balb/c-derived 4T1 mammary tumor cell line to study tumor metastasis because 4T1 cells and human mammary adenocarcinomas share similar sites of metastasis (Aslakson and Miller, 1992; Dexter et al., 1978; Miller et al., 1983). Human breast cancer spreads first to the lungs in 24%–77% of the cancers and to the liver in 22%–62% (Kamby et al., 1987; Rutgers et al., 1989; Tomin and Donegan, 1987). Similarly, 4T1 spreads in mice to the lungs and liver in >95% and >75% of the cancers, respectively (Pulaski and Ostrand-Rosenberg, 1998). We used the 4T1 cells to prepare a cDNA library enriched in transcripts that encode secreted and transmembrane proteins potentially involved in metastasis.

The 4T1 phage library was injected intravenously, and phage that localized to the lungs were isolated. After three rounds of selecting for lung-homing phage clones, 32 clones were initially isolated. We tested individual phage clones for their ability to specifically bind to lung vasculature. One of the five lung-specific clones we identified encoded a fragment of a protein recently deposited into GenBank (accession numbers AAL92861 and AAP30791).

The selected phage, when intravenously (i.v.) injected into mice and allowed to circulate for 5 min, bound to lungs almost 20-fold more than control phage (Figure 1A). In contrast, similar numbers of the selected phage and control phage accumulated in pancreas, breast, skin, kidney, brain, and liver. When injected into the left ventricle of the heart in mice, significantly more selected phage accumulated in the lungs, pancreas, kidney, brain, and liver than control phage (Figure 1B). Similar numbers of selected phage and control phage accumulated in breast, skin, and bone. The selected phage colocalized with blood vessels in the lungs (Figure 1C).

cDNA cloning and membrane topology of metadherin
The deduced amino acid sequence of the lung-homing domain of the lung-homing phage is shown in Figure 2A. Using BLAST

(Altschul et al., 1997), we found one cDNA clone (GenBank accession number AY082966) that encoded the putative full-length human protein corresponding to the phage clone. The GenBank entry refers to the protein as "LYRIC" and describes it as a putative CEACAM1-associated protein in colon carcinoma. These observations remain unpublished. Based on our results
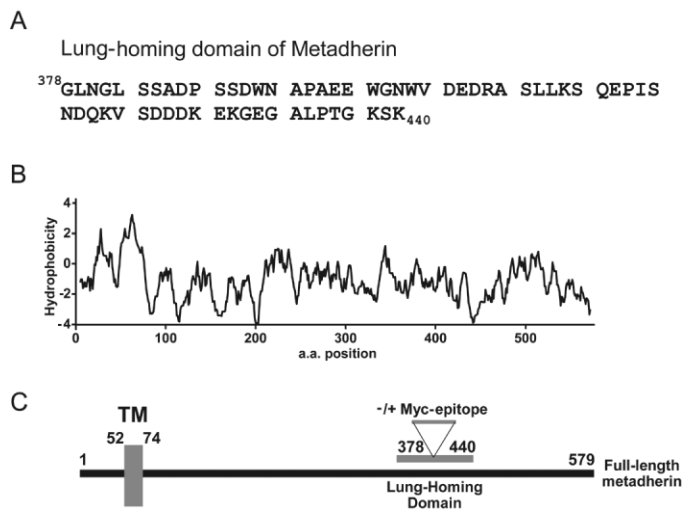

Figure 2. Sequence analysis of metadherin

A: Amino acid sequence of metadherin's lung-homing domain. This domain corresponds to residues 378–440 of the full-length mouse metadherin protein.
B: Hydrophobicity analysis of metadherin, using a window size of 9 amino acids.
C: Layout of the full-length metadherin protein. TM denotes the location of the putative transmembrane domain. The numbers denote the position of amino acids in the metadherin protein.
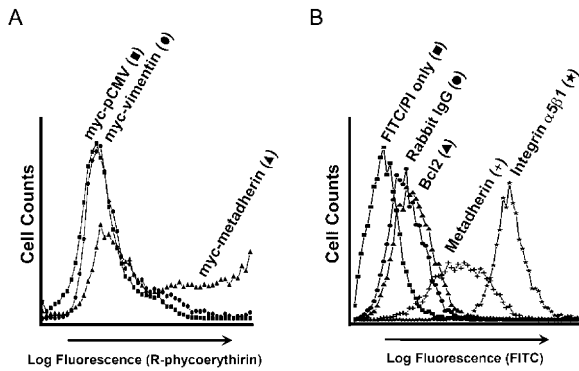
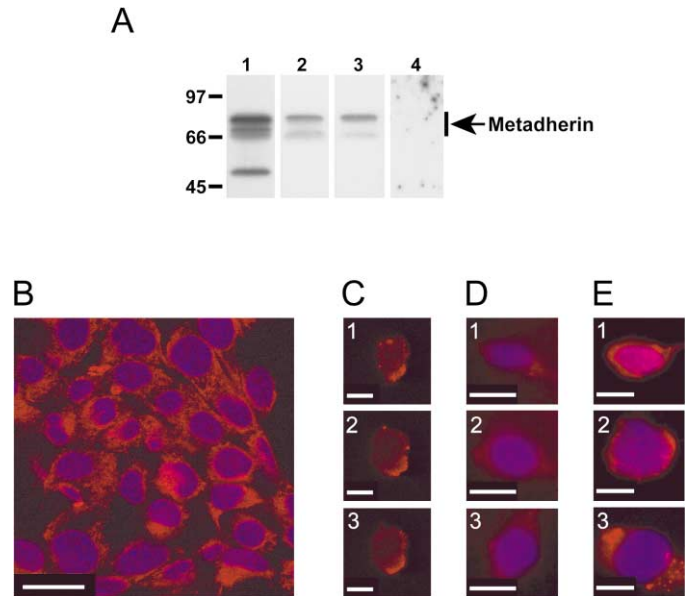**Figure 3.** Lung-homing domain of metadherin is extracellular

A: HEK293T cells expressing full-length myc-tagged metadherin, myc-vimentin, or myc-pCMV were analyzed by flow cytometry. Anti-myc antibodies were applied to the cells and detected with a PE-labeled secondary Ab.
B: Rabbit IgG, anti-Bcl2 polyclonal Ab (Bcl2), anti-integrin α5β1 polyclonal antibody (Integrin α5β1), or anti-metadherin$_{(378-440)}$ (metadherin) was applied to nonpermeabilized 4T1 tumor cells and detected with a FITC-labeled secondary Ab. Control cells were stained with FITC-labeled secondary Ab and propidium iodide alone (FITC/PI only).

Figure 4. Metadherin expression in 4T1 tumor cells

A: Immunoblot of endogenous metadherin. Lanes 1 and 4, 4T1 cell extract; lane 2, KRIB cell extract; lane 3, MDA-MB-435 cell extract. Immunoblot detection of metadherin was performed with anti-metadherin$_{(378-440)}$ (lanes 1–3). Immunoblot detection of an unrelated protein, Clone D2, was performed with anti-Clone D2 polyclonal antibody (lane 4).
B: Confocal projection of permeabilized 4T1 cells stained with anti-metadherin$_{(378-440)}$. Scale bar corresponds to 50 μm.
C: Confocal sections (0.15 μm thick; panels 1–3) of nonpermeabilized 4T1 cells stained with anti-metadherin$_{(378-440)}$.
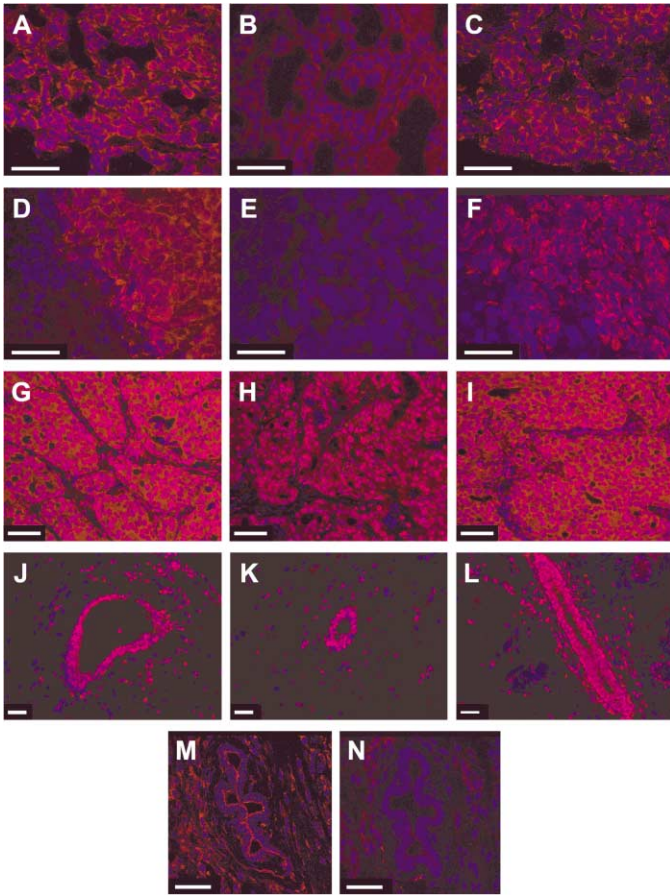**D and E:** Nonpermeabilized 4T1 cells stained with anti-metadherin$_{(378-440)}$ that was pre-incubated with excess metadherin$_{(378-440)}$ peptide (**D**, panels 1–3) or excess control peptide (**E**, panels 1–3). In **B–E**, anti-metadherin$_{(378-440)}$ was detected with Alexa 594 goat anti-rabbit IgG antibody (red). Nuclei were stained with DAPI (blue). Images in **D** and **E** were captured using an inverted fluorescent microscope. The scale bars in **C–E** correspond to 5 μm.

that show the importance of this lung-homing protein in breast cancer metastasis, we have named this protein metadherin (metastasis adhesion protein). We used a reported mouse cDNA homolog of metadherin (GenBank accession number AK029915) to design oligonucleotides and amplified the full-length 1740 bp mouse metadherin cDNA by reverse transcription-polymerase chain reaction.

Analysis of the hydrophobic regions of metadherin (Kyte and Doolittle, 1982) revealed that amino acid residues 52–74 encode a putative transmembrane domain (Figure 2B). We did not find any domains in metadherin that were similar to other known proteins. Using a hidden Markov model to detect membrane helices and predict transmembrane topology in proteins (Glasgow, 1998; Krogh et al., 2001), we found that metadherin was predicted to be a type II transmembrane protein with an extracellular lung-homing domain. To confirm this prediction, we subcloned a c-*myc* epitope into the lung-homing domain of the metadherin cDNA, as shown in Figure 2C. This myc-tagged cDNA was expressed in HEK293T cells, and these cells were then stained with anti-myc antibodies. Using flow cytometry, we observed that intact myc metadherin-expressing cells were labeled with anti-myc antibodies (Figure 3A), indicating that the lung-homing domain of metadherin was extracellular. No cell surface labeling was detected in vector-transfected cells or nonpermeabilized cells expressing the intracellular protein myc-vimentin (Figure 3A). Anti-myc antibodies stained the myc vimentin-expressing cells when permeabilized, which confirms the expression of myc-vimentin, and permeabilized cells expressing vector alone were not stained with anti-myc antibodies (data not shown).

Metadherin expression in tumor cells and tumors

We also raised rabbit antibodies reactive to the lung-homing domain of metadherin to study endogenous metadherin in tumor cells and tumors. These antibodies bound to nonpermeabilized 4T1 cells in flow cytometry (Figure 3B). This result confirms the presence of the lung-homing domain of metadherin on tumor

cells at the cell surface where it would be available to bind to vascular targets during metastasis. An antibody against a cytoplasmic protein (Bcl-2) and rabbit IgG did not bind to the surface of nonpermeabilized 4T1 cells, while the cells were strongly positive for integrin α5β1 (Figure 3B).

In 4T1 tumor cell extracts, anti-metadherin$_{(378-440)}$ detected proteins with apparent molecular weights of approximately 80 kDa, 75 kDa, and 55 kDa (Figure 4A, lane 1). KRIB and MDA-MB-435 cell extracts also contained the 80 kDa and 75 kDa proteins (Figure 4A, lanes 2 and 3, respectively). A control, affinity-purified polyclonal antibody reactive to a nonrelated protein (Clone D2) did not detect the anti-metadherin$_{(378-440)}$ immunoreactive bands (Figure 4A, lane 4). The 80 kDa and 55 kDa proteins detected by anti-metadherin$_{(378-440)}$ were also produced by an in vitro transcription and translation reaction using an epitope-tagged metadherin cDNA as template (data not shown); this suggests that the 55 kDa protein may be a degradation product of metadherin.

In fixed and permeabilized 4T1 cells, metadherin immunoreactivity localized throughout the cytoplasm (Figure 4B). In nonpermeabilized cells, the staining was concentrated at the edges of the cells (Figure 4C). Controls showed that pre-incubation of anti-metadherin$_{(378-440)}$ with the metadherin$_{(378-440)}$ lung-homing

Figure 5. Metadherin expression in tumor xenografts and human breast cancer

MDA-MB-435 breast adenocarcinoma (**A–C**) or KRIB osteosarcoma (**D–F**) tumor xenografts grown in nude Balb/c mice were analyzed by immunostaining. Sections were stained with either anti-metadherin$_{(378-440)}$ alone (**A and D**) or anti-metadherin$_{(378-440)}$ pre-incubated with excess metadherin$_{(378-440)}$ peptide (**B and E**) or excess control peptide (**C and F**). Sections of human breast tumor (**G–I**) or normal human breast tissue (**J–L**) were stained with either anti-metadherin$_{(378-440)}$ alone (**G and J**) or anti-metadherin$_{(378-440)}$ pre-incubated with excess metadherin$_{(378-440)}$ peptide (**H and K**) or excess control peptide (**I and L**). Sections of mouse breast tissue were stained with either anti-metadherin$_{(378-440)}$ alone (**M**) or anti-metadherin$_{(378-440)}$ pre-incubated with excess metadherin$_{(378-440)}$ peptide (**N**). In all panels, anti-metadherin$_{(378-440)}$ was detected with Alexa 594 goat anti-rabbit IgG antibody (red) and nuclei were stained with DAPI (blue). The confocal projections in **A–N** were captured using a confocal microscope. The scale bars correspond to 50 μm.

peptide inhibited the staining (Figure 4D), whereas a control peptide did not (Figure 4E).

We detected strong metadherin staining in sections of MDA-MB-435 and KRIB tumor xenografts (Figures 5A and 5D), which are two tumor models known to generate lung metastases (Berlin et al., 1993; Price et al., 1990). The anti-metadherin immunostaining was specific, since pre-incubation of antibody with the metadherin$_{(378-440)}$ lung-homing peptide (Figures 5B and 5E) inhibited the staining and control peptide (Figures 5C and 5F) had no inhibitory effect. Subcutaneous tissue or skin adjacent to the tumors showed no anti-metadherin staining (e.g., Figure 5D, lower left corner).

Several human breast cancer sections stained with anti-

metadherin$_{(378-440)}$ showed high amounts of metadherin throughout the tumor (Figure 5G). In contrast, we did not detect any cytoplasmic or cell surface-associated metadherin in normal human breast tissue, but nuclear staining was present (Figure 5J). The cell surface staining of breast cancer tissue could be inhibited with the metadherin$_{(378-440)}$ peptide (Figure 5H), but not with control peptide (Figure 5I). Neither peptide inhibited nuclear staining (Figures 5H, 5I, 5K, and 5L). The human sections were paraffin embedded and processed with heat-induced target retrieval. Apparently, the antibody nonspecifically stains nuclei in such sections. In frozen tissue sections of normal mouse mammary tissue, we found specific metadherin staining at the apical surface of epithelial cells lining ducts of the mammary glands (Figures 5M and 5N), and a small amount of metadherin was dispersed through the mammary fat pad. We detected no metadherin in the spleen, kidney, lung, or skin, but minute amounts were seen in the liver. Purkinje neurons in the early postnatal and adult cerebellum were strongly positive for metadherin staining (data not shown). Tissue array slides of human breast tissue and breast adenocarcinomas were also stained with anti-metadherin$_{(378-440)}$. We detected strong anti-metadherin$_{(378-440)}$ staining throughout the tissue sections in 17 out of 31 breast adenocarcinomas, while metadherin was absent in 18 out of 20 samples of normal breast tissue. The other two normal breast tissue samples stained positive for metadherin at epithelial cells lining ducts of the mammary glands. These immunostaining results show that metadherin is selectively overexpressed in tumors.

Effect of metadherin expression on the localization of injected cells

To test the effect of metadherin on tissue distribution of i.v.-injected tumor cells, we studied HEK293T cells transiently transfected with metadherin. The cells were cotransfected with DsRed2 and metadherin, and DsRed2-positive cells were isolated using fluorescence-activated cell sorting (FACS). The cells were then i.v.-injected into mice. Fluorescent cells were detected in the blood vessels of lungs examined 2 hr after the injection; cell counting showed 22% more metadherin-transfected cells than that of vector-transfected cells (Figures 6A and 6B; Student's t test; p < 0.001). We did not see significant numbers of DsRed2 HEK293T cells in the brain, skin, liver, kidney, heart, spleen, or pancreas (Figure 6A). This result supports the phage homing data indicating that metadherin preferentially binds to lung vasculature. The relatively small incremental effect of metadherin overexpression on the lung localization of HEK293T cells is probably due to endogenous expression of metadherin by these cells, which immunoblotting showed to be about 45% of that in the 4T1 cells (data not shown).

Anti-metadherin and metadherin siRNA inhibit 4T1 lung metastasis

To gain information on the role of metadherin in metastasis, we decided to inhibit metadherin activity in the 4T1 cells with antibodies reactive to the lung-homing domain of metadherin. When co-injected with the 4T1 cells, anti-metadherin$_{(378-440)}$ inhibited lung metastasis by about 40% (Figure 7, p < 0.01), compared to 4T1 cells treated with rabbit IgG. In a separate experiment, we did not observe any difference between the growth of mammary fat pad tumors formed from 4T1 cells pretreated with the anti-metadherin$_{(378-440)}$ or rabbit IgG (data not shown).
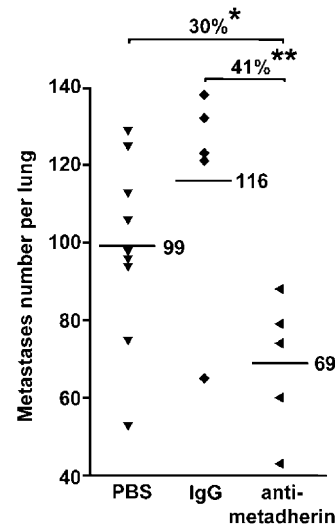
A

B
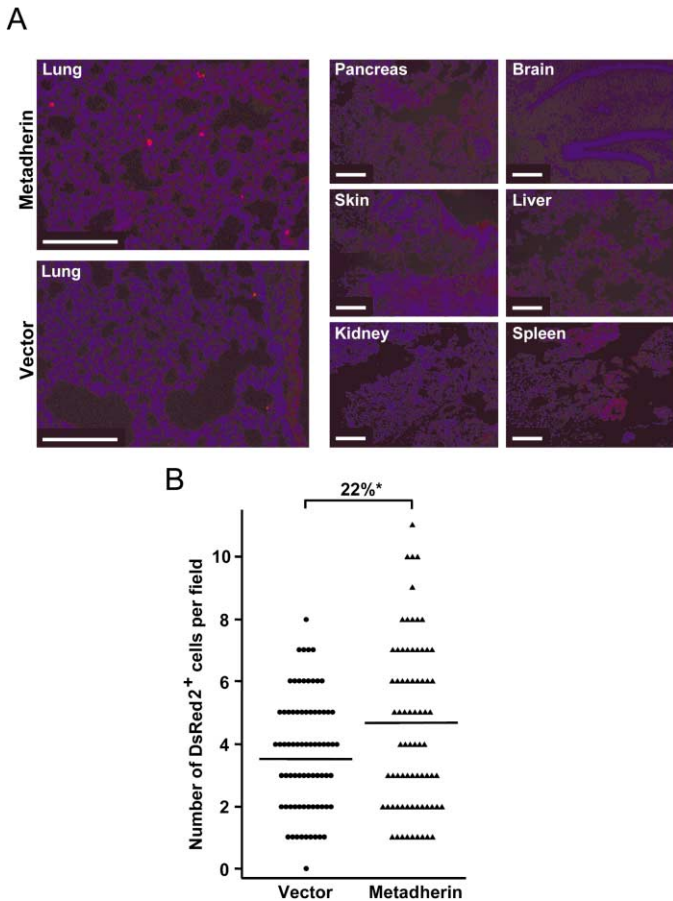
Figure 6. HEK293Ts overexpressing metadherin localize to lung

A: DAPI-stained (blue) lung sections from mice injected with HEK293T cells that were cotransfected with a DsRed2 expression vector (red) and either metadherin-pCMV or expression vector alone. Pancreas, skin, kidney, brain, liver, and spleen sections from mice injected with HEK293T cells that were transfected with a DsRed2 expression vector (red) and metadherin-pCMV. The scale bars correspond to 100 μm.

B: Number of DsRed2-positive cells per viewing field in the lung sections (n = 75; one-tailed Student's t test; *p < 0.001).

**Figure 7.** Anti-metadherin antibodies inhibit lung metastasis

Number of lung metastases from mice injected with 4T1 cells that were treated with anti-metadherin$_{(378-440)}$, rabbit IgG, or PBS. Average number of metastases in each group is denoted with a horizontal line. The percent difference in average number of metastases between groups is denoted above the brackets, with significance measured using a one-tailed Student's t test (*p < 0.02, **p < 0.01).

As a second approach, we measured the metastatic potential of breast cancer cells expressing reduced levels of metadherin. As shown in Figure 8A, siRNA reactive to metadherin, but not siRNA to GAPDH or scrambled-siRNA, was able to knock down expression of transfected myc-metadherin in HEK293T cells. We were unable to generate stable cell lines that expressed reduced levels of metadherin because metadherin expression levels returned to normal after 2 weeks. Instead, we coexpressed green fluorescent protein (EGFP) and the metadherin-reactive siRNA or scrambled-siRNA in 4T1 cells and selected for siRNA-transfected cells by FACS. The transfection with metadherin-siRNA did not affect the expression of β-actin or the type II transmembrane protein, transferrin receptor (Figure 8B). However, metadherin protein expression in metadherin-siRNA cells was reduced by about 40% relative to the scrambled-siRNA cells (Figure 8B). Measured by real-time PCR, metadherin-siRNA cells expressed about 40% less metadherin mRNA than the scrambled-siRNA cells, when metadherin mRNA levels were normalized to β-actin mRNA levels (Figure 8C).

Using flow cytometry, the effects of metadherin-reactive siRNA and scrambled-siRNA on cell growth and viability were assessed. In 4T1 cells cotransfected with EGFP and metadherin-reactive siRNA or scrambled-siRNA expression plasmids, we did not detect any significant difference in propidium iodide staining between the EGFP-positive populations from the metadherin-reactive siRNA or scrambled-siRNA cells (4.52% versus 5%, see Supplemental Figure S1 at http://www. cancercell.org/cgi/content/full/5/4/365/DC1). This suggested metadherin-reactive siRNA did not affect 4T1 cell viability under these conditions. In addition, the number of EGFP-positive cells in the metadherin-reactive siRNA and scrambled-siRNA transfected 4T1 cells was not significantly different, suggesting the metadherin-reactive siRNA plasmid did not inhibit cell growth during the 2 day transfection period (9.55% versus 9.95%, Supplemental Figure S1). Also, we counted the number of cells before and 2 days after transfecting the siRNA expression plasmids and did not see any significant effect of the metadherin-siRNA on the growth rate of the cells (data not shown).

Immunostaining confirmed that metadherin-siRNA cells expressed less metadherin (Figure 8D, 1 and 2) than scrambled-siRNA cells (Figure 8D, 3 and 4). Using FACS, we isolated EGFP-positive cells that excluded propidium iodide to select for viable siRNA-transfected cells (Figure 8D, 5–8). When injected into mice, the 4T1 cells expressing metadherin-reactive siRNA formed about 80% fewer experimental lung metastases than cells expressing scrambled-siRNA (Figure 8E, Student's t test, p < 0.001).

Discussion

We report here that a protein, metadherin, is overexpressed in breast tumors and binds to lung vasculature through a C-ter-
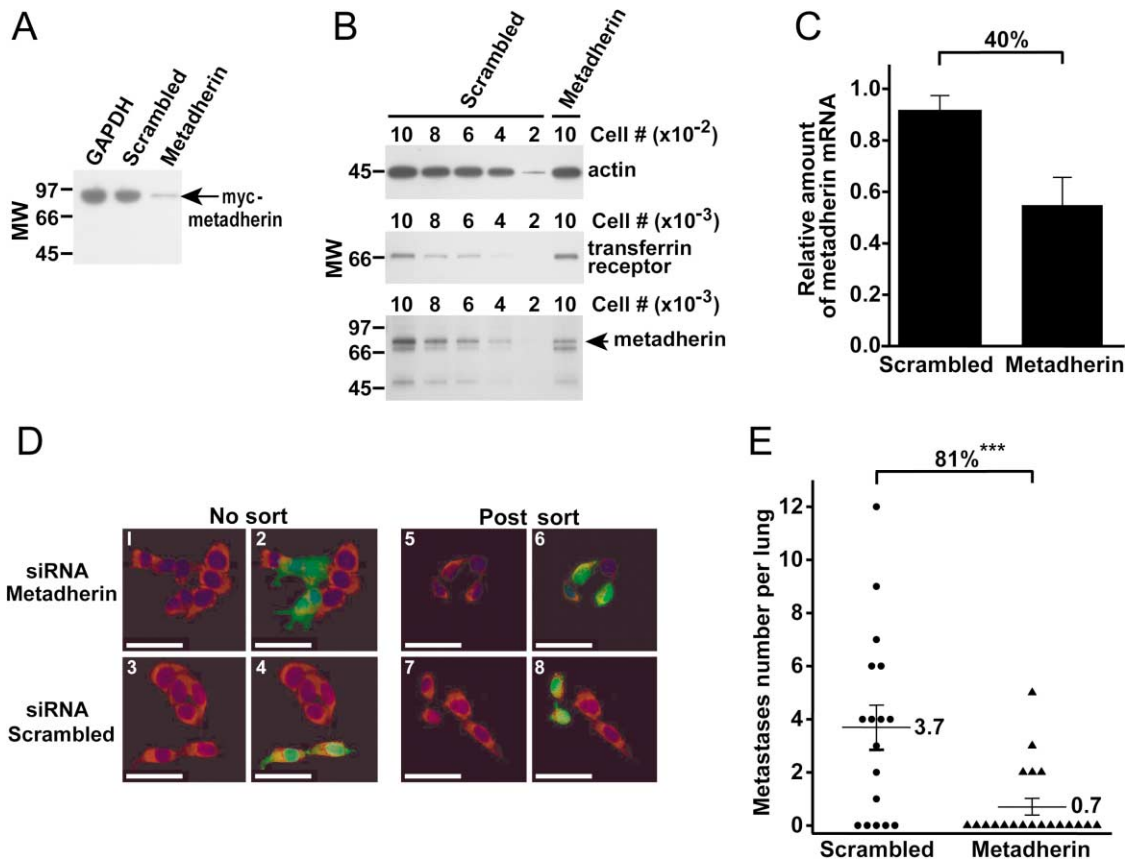
Figure 8. siRNA reactive to metadherin mRNA inhibits lung metastasis

A: Anti-myc immunoblot of HEK293T cell extracts expressing myc-tagged metadherin and siRNA reactive to GAPDH or metadherin, or scrambled-siRNA.

B: Immunoblot quantitation of β-actin, transferrin receptor, or metadherin protein levels in 4T1 cells expressing siRNA reactive to metadherin or scrambled-siRNA. The arrow in **B** denotes the 80 kDa metadherin protein band quantified by densitometry.

C: Quantitation of metadherin mRNA in 4T1 cells expressing siRNA reactive to metadherin or scrambled-siRNA. The relative amount of metadherin mRNA was normalized to the abundance of β-actin mRNA, also detected by real-time PCR. Error bars represent mean ± SD.

D: 4T1 cells were cotransfected with an EGFP expression vector and a vector expressing siRNA reactive to metadherin (panels 1, 2, 5, and 6) or scrambled-siRNA (panels 3, 4, 7, and 8). The cells were sorted by FACS to select for EGFP-expressing cells (Post sort). Nonsorted cells (No sort; panels 1–4) and postsorted cells (panels 5–8) were stained with anti-metadherin$_{(378-440)}$. Panels 2, 4, 6, and 8 show the EGFP-expressing cells (green) displayed in panels 1, 3, 5, and 7, respectively. In all panels, anti-metadherin$_{(378-440)}$ was detected with Alexa 594 goat anti-rabbit IgG antibody (red). Nuclei were stained with DAPI (blue). The scale bars correspond to 50 μm.

E: siRNA reactive to metadherin transcripts inhibits 4T1 cell experimental lung metastasis. Values are expressed as the number of tumor foci per 10,000 cells injected. Bars represent mean ± SEM (one-tailed Student's t test; ***p < 0.001). In **C** and **E**, percentages indicate relative suppression compared to control group.

minal segment in the extracellular domain. We also show that blocking the lung-homing domain with antibodies or inhibiting the expression of metadherin with siRNA can inhibit breast cancer metastasis. These results identify metadherin as a potential mediator of cancer metastasis.

Metadherin appears to detect a specific marker of lung vasculature. Metadherin phage accumulated in lung vasculature after either tail-vein or intracardiac injection, suggesting that among the various vascular beds, it primarily binds to lung endothelium. In this regard, metadherin is similar to lung-specific homing peptides isolated by in vivo phage display (Rajotte and Ruoslahti, 1999) and antibodies that specifically bind to lung vasculature (McIntosh et al., 2002). The ability of metadherin phage to specifically target lung vasculature suggests that among the various vascular beds, the molecule(s) metadherin binds ("metadherin receptor") is primarily expressed on lung endothelium. The identity of the receptor is currently unknown.

Tissue-specific expression of vascular markers is not limited to lung vasculature; recent data suggest that each tissue puts a specific signature on its vasculature (Ruoslahti, 2002). Thus, the binding of tumor cells to tissue-specific vascular markers may play a role in selective tumor metastasis to other tissues as well.

Metadherin appears to primarily mediate metastasis to one of the four sites commonly affected by human breast cancer: the lungs. The fact that metadherin phage primarily targeted the lungs after either intravenous or intracardiac injection and was not detected in substantial amounts in the liver, brain, or bone suggests that metadherin mediates specific adhesion to lung vasculature, even after passing through capillary networks of other organs. The ability of metadherin phage to accumulate in the lungs even after intracardiac injection suggests that metadherin also promotes selective binding of tumor cells to lung

vasculature, rather than helping them adhere to the first capillary bed the cells encounter.

Metadherin may be important to the pathogenesis of cancer. We found high expression of metadherin in cultured tumor cells, and its expression was higher in both experimental and clinical breast cancers than in normal breast tissue and in other normal tissues, as detected with specific metadherin antibodies. The only exception to the relatively low expression in the normal tissues we studied were the Purkinje cells in the cerebellum; metadherin may have a specific function in these cells.

A recent gene expression profiling study on breast cancer patients revealed that metadherin is overexpressed in many metastatic breast cancers. van 't Veer et al. (2002) found that metadherin mRNA expression levels (described as GenBank entry AK000745) in breast cancer patients were significantly correlated with a poor prognosis due to metastasis. Out of 25,000 genes analyzed, metadherin was ranked 25th when correlating gene expression levels with metastasis. Most of the patients who expressed high levels of these "poor prognosis" classified genes developed distant metastases within 5 years of observation. Thus, metadherin is overexpressed in breast cancer both at the protein and mRNA levels and is associated with increased malignancy of these cancers. Our results suggest that the association of metadherin overexpression with poor prognosis of breast cancer is due to an ability of metadherin to specifically promote tumor metastasis to the lungs.

There are other examples of adhesive interactions that are required in order for lung metastases to form. Dipeptidyl dipeptidase IV on lung endothelial cells was found to be an adhesion receptor for fibronectin on metastasizing breast and prostate carcinoma cells in a mouse model (Cheng et al., 1998; Johnson et al., 1993). In another mouse model, Ca^{2+}-sensitive chloride channel, hCLCA2, expressed on lung endothelial cells was reported to be a ligand for β4 integrins on metastasizing breast cancer cells (Abdel-Ghany et al., 2001; Elble et al., 1997). Most recently, the secreted chemokine, CXCL12, which is highly expressed in the lung, liver, and lymph nodes, was shown to bind to CXCR4 receptors on the surface of metastasizing breast cancer cells (Muller et al., 2001). Moreover, interfering with only one of these interactions was sufficient to inhibit metastasis (Abdel-Ghany et al., 2001; Cheng et al., 1998; Muller et al., 2001). Although there is no evidence available on the significance of these interactions in breast cancer, it seems that multiple interactions of cell adhesion molecules and growth factor receptors may be required for the attachment and growth of circulating tumor cells in the lung. Similar mechanisms based on unique vascular addresses may play a role in organ-specific metastasis to other organs.

The importance of metadherin in tumor cell metastasis might not only be limited to breast cancer. Using SAGEmap (Lal et al., 1999; Lash et al., 2000), a component of The Cancer Genome Anatomy Project at the National Center for Biotechnology Information, we found that metadherin is significantly overexpressed not only in breast cancers, but also in cancers of the brain and prostate (p < 0.05). This suggests that metadherin might also play a role in the metastasis of these cancers. Metadherin is conserved among mammals, and with the BLAST algorithm (Altschul et al., 1997), we found additional mouse and human metadherin-like molecules in the GenBank databases. It will be important to determine what role, if any, these related molecules might play in cancer.

Metadherin is a potential target for tumor diagnosis and preventative therapy. Given the cell surface localization of metadherin in tumor cells and the discrete overexpression of metadherin in primary tumors, therapeutics that target metadherin might prove to be selective for metastasis-prone tumors. Our results showing the antimetastatic activity of anti-metadherin antibodies and siRNA reactive to metadherin mRNA suggest that antibody or siRNA-based therapies that target metadherin might be effective in preventing certain tumors from metastasizing.

Experimental procedures

Cell lines, mice, and tumors

4T1, a cell line derived from a Balb/c breast adenocarcinoma, was obtained from ATCC and maintained as described by Pulaski and Ostrand-Rosenberg (1998). MDA-MB-435 and KRIB cell lines were maintained as described before (Laakkonen et al., 2002). Nude Balb/c mice were subcutaneously injected with 1×10^6 tumor cells and kept for 5 weeks (KRIB) or 10 weeks (MDA-MB-435). Tumors were then removed, frozen in OCT embedding medium (Tissue-Tek, Elkhart, IN), and sectioned. The Burnham Institute Animal Research Committee approved the animal experimentation.

Phage library and screening

A cDNA library was prepared from membrane bound polyribosomal mRNA of 4T1 cells. Briefly, RNA from membrane bound polysomes of 3.2×10^8 4T1 cells was prepared using the methods described by Mechler (1987). Approximately 1 μg of this RNA was used to generate 6 μg of amplified antisense mRNA (aRNA), using the methods described by Luo et al. (1999). Using aRNA as template, mRNA was synthesized as described by Luo et al. (1999), except the primer, 5′-TTNNNNNN-3′, was used instead of random hexamer primer, and methylated dNTPS were used instead of dNTPs. A cDNA library was prepared from the mRNA, as described in the manufacturer's protocol (OrientExpress Random Primer cDNA synthesis kit; Novagen, Madison, WI).

T7 phage vectors, designed to express cDNA library-encoded proteins fused at the N terminus to phage 10B coat protein and to a myc epitope at the C terminus, were then assembled. Oligonucleotides encoding myc epitopes in all three reading frames, internal EcoRI and HindIII restriction enzyme cleavage sites and flanking EcoRI/HindIII adapters, were synthesized. The oligonucleotides were then individually phosphorylated, annealed, and ligated to EcoRI/HindIII-digested T7Select 1-2a, 1-2b, or 1-2c vector arms (Novagen) to generate myc epitope phage vectors.

To prevent myc epitope expression in phage vectors that were unsuccessfully ligated to cDNA during library construction, a linker encoding stop codons in all three reading frames was inserted upstream of the myc epitope and downstream of the 10B coat protein in the phage vector. Oligonucleotides encoding stop codons in all three reading frames were synthesized, phosphorylated, annealed, and ligated to EcoRI/HindIII-digested myc epitope phage vectors to form myc-T7 vectors. A map of the myc epitope phage vector is shown in Supplemental Figure S2 at http://www.cancercell.org/cgi/content/full/5/4/365/DC1. The cDNA libraries were then ligated to EcoRI/HindIII-digested myc-T7 vector, phage were packaged, and libraries were amplified in E. coli BLT5615 cells (according to the manufacturer's protocol; Novagen). As measured by plaque assay, the library contained 4.7×10^6 primary recombinants.

Phage clones that expressed cDNA inserts with open reading frames were enriched by three rounds of selection with anti-myc mAb (3.1 μg/ml MAB8864; Chemicon, Temecula, CA) bound to rat anti-mouse IgG1 magnetic beads (3.1 μl per 1 ml of buffer; Miltenyi Biotec, Auburn, CA). Selections were performed with 10^{11} plaque forming units (pfu) of phage in 10 ml of Dulbecco's phosphate buffered saline containing 0.5% bovine serum albumin (PBSB). Phage were applied to a magnetized LS MACS column (Miltenyi Biotec), washed with buffer (50 mM Tris-HCl [pH 7.5], 150 mM NaCl, 1% NP-40, 0.5% sodium deoxycholate, 0.1% sodium dodecyl sulfate), eluted with PBSB after demagnetizing the column, and transferred to a second column for more washes. Phage were amplified in BLT5615 E. coli using the liquid lysate method after each anti-myc selection round and supernatants clarified by centrifugation were supplied with 1% vol/vol of E. coli protease

inhibitors cocktail (P-8465; Sigma-Aldrich, St. Louis, MO). After three rounds of myc antibody sorting, over 90% of the phage clones in the 4T1 library were found to contain open reading frame cDNA inserts. On average, the phage clones expressed protein fragments that were 75 amino acids long.

Ex vivo and in vivo screenings with the 4T1 phage library were performed as previously described (Hoffman et al., 2004). Briefly, cell suspensions were prepared from mouse lungs and incubated overnight at 4°C with 10^9 pfu of 4T1 phage library. The cells were washed to remove unbound phage, and the bound phage were rescued and amplified by adding BLT5615 *E. coli*. The amplified 4T1 phage library was applied to a lung cell suspension for a second ex vivo selection round, as before. The ex vivo preselected phage pool (200 μl, or approximately 10^9 pfu) was injected intravenously into 2-month-old Balb/c mice through the tail vein, allowed to circulate for 5 min, and heart-perfused with PBS to remove unbound intravascular phage. Cell suspensions of tissue were prepared by mechanical disruption and washed to remove unbound phage, and the bound phage were rescued and amplified by adding BLT5615 *E. coli*. The phage pool was reinjected into Balb/c mice, and the cycle repeated twice. For each selection round, the number of phage recovered from the tissue was normalized to the number of injected phage and tissue mass. After three rounds of in vivo selections, cDNA inserts were sequenced from 32 phage clones as described before (Hoffman et al., 2004).

Cloning of full-length metadherin cDNA

The following primers were synthesized to amplify the full-length mouse metadherin cDNA: 5′-ACCATGGCTGCACGAAGCTGGCAGGACGAGCTG-3′ and 5′-TCACGTTTCCCGTCTGGCCTTTTTCTTCTTTTTTA-3′. RNA was isolated from 4T1 cells using a Total RNA Isolation Kit (Qiagen, Valencia, CA). The metadherin cDNA was amplified by RT-PCR using a Superscript One-Step RT-PCR Kit for Long Templates (according to manufacturer's protocol; Invitrogen, Carlsbad, CA) and subcloned into the TOPO-TA vector, pcDNA3.1-V5/His (according to the manufacturer's protocol; Invitrogen).

A myc epitope was added to metadherin protein by first inserting an *Eco*RI restriction enzyme site in the metadherin cDNA after nucleotide 1222 with a QuickChange site-directed mutagenesis kit (Stratagene, La Jolla, CA). Then, oligonucleotides encoding a myc epitope (EQKLISEEDL) and flanking *Eco*RI adapters were synthesized, phosphorylated, and ligated into the *Eco*RI-digested metadherin cDNA. The myc-metadherin cDNA was subcloned into the pCMV vector (Clontech, Palo Alto, CA). Human myc-vimentin cDNA was generated by reverse transcription-polymerase chain reaction, using vimentin-specific primers and human mRNA as template, and then subcloned into the pCMV-Myc vector (Clontech, Palo Alto, CA).

Antibodies, immunoblotting, and immunohistology

Anti-T7 phage affinity purified antibody was previously described (Laakkonen et al., 2002). A polyclonal antibody was generated in New Zealand White rabbits against the recombinant metadherin lung-homing domain that was fused to glutathione-S transferase. The initial immunization was done in complete Freund's adjuvant and boosters were with incomplete Freund's adjuvant. The antibody was affinity purified on recombinant hexahistine-tagged metadherin(378-440) peptide coupled to SulfoLink Gel (Pierce, Rockford, IL) via a cysteine residue added to the amino terminus of the metadherin(378-440) peptide.

Blood vessel localization of metadherin phage was examined by i.v. injection of 2.5×10^{10} pfu metadherin phage (in 200 μl M9LB) into the tail vein of a mouse. Blood vessels were visualized by co-injection of phage with 200 μg of *Lycopersicon esculentum* (tomato) lectin conjugated to fluorescein. The injected materials were allowed to circulate for 10 min. Lungs were removed and frozen in OCT embedding medium (Tissue-Tek).

Tumor cell lysates were prepared in 2.5× Laemmli's sample buffer (Laemmli, 1970) at a ratio of 10^6 cells per 150 μl and subjected to SDS-PAGE on 4%–20% acrylamide gradient gels. Proteins were transferred to PVDF membrane and immunoblots were performed with anti-metadherin(378-440) (0.1 μg/ml) and goat anti-rabbit IgG-HRP (diluted 1:10,000; Bio-Rad, Hercules, CA) and developed using ECL+plus chemiluminescence reagent (Amersham Biosciences, Piscataway, NJ), according to the manufacturer's instructions. The relative amount of metadherin detected by immunoblot was quantitated using an AlphaImager (Alpha Innotech, San Leandro, CA). β-actin was detected with an anti-actin monoclonal antibody (10 μg/ml, Chemicon). Transferrin receptor was detected with an anti-transferrin receptor polyclonal antibody (2 μg/ml, Santa Cruz Biotech, Santa Cruz, CA). Affinity-purified

polyclonal antibody reactive to a 175 kDa protein, Clone D2, was prepared as described for anti-metadherin(378-440). Control immunoblots were performed with anti-Clone D2 (0.1 μg/ml) and goat anti-rabbit IgG-HRP (described above).

For cell surface labeling, anti-metadherin(378-440), diluted to 20 μg/ml in ice-cold IMEM (Invitrogen) with 10% fetal bovine serum (FBS), was added to cells cultured on chamber slides and incubated for 1 hr on ice. The cells were washed with IMEM and fixed with cold 4% parformaldehyde in PBS for 15 min. Anti-metadherin antibodies were detected with Alexa 594 goat anti-rabbit IgG (diluted 1:500 in PBS with 1% FBS and 3% goat serum). Slides were mounted with Vectashield fluorescence mounting medium (Vector, Burlingame, CA). For permeabilized cell labeling, cells were first fixed with 4% parformaldehyde (described above) and then treated with 0.1% Triton X-100 in PBSB for 15 min. The cells were washed with PBSB and incubated with anti-metadherin(378-440) (diluted to 20 μg/ml in IMEM with 10% FBS) for 1 hr at room temperature. Anti-metadherin(378-440) was detected with Alexa 594 goat anti-rabbit IgG, as described above.

Paraffin-embedded human tissue sections (Spring Biosciences, Fremont, CA) and breast adenocarcinoma tissue array sections (InnoGenex, San Ramon, CA; NCI, Frederick, MD) were deparaffinized and then treated with Target Retrieval Solution (according to the manufacturer's instructions; DAKO, Carpinteria, CA). For immunofluorescence imaging, the sections were stained as described above, except PBSB was substituted for 0.5% Blocking Reagent (NEN Life Sciences, Boston, MA) in 0.1 M Tris/150 mM NaCl. The tissue array sections were stained as described above, except anti-metadherin(378-440) was detected with the EnVision + System (according to the manufacturer's instructions; DAKO) and cells were counterstained with hematoxylin (DAKO). To determine specificity, anti-metadherin(378-440) (20 μg/ml) was pre-incubated overnight with 200 μg/ml recombinant metadherin lung-homing protein or unrelated recombinant control protein (72 amino acid, lung-homing Clone D2) in blocking buffer before immunostaining the sections.

FACS analysis

Transiently transfected HEK293T cells expressing myc-vimentin, myc-metadherin, or myc-pCMV vector alone (Clontech) were detached from their culture dishes by gently washing with PBS containing 1% BSA (PBSB). The cells were then stained with anti-myc mAb (2 μg/ml in PBSB; Chemicon) for 20 min at 4°C. The cells were washed with PBSB, stained with goat anti-mouse IgG PE-labeled antibody (4 μg/ml in PBSB; Pharmingen, San Diego, CA), washed again with PBSB, fixed with 2% parformaldehyde in PBS, resuspended in PBS, and analyzed using a FACScan flow cytometer (BD, San Jose, CA).

To analyze the 4T1 cells by FACS, the cells were detached from culture plates by incubating with PBS with 2 mM EDTA (PBSE) for 10 min. The cells were then washed with PBSB and incubated with 40 μg/ml (in PBSB) of the following antibodies: anti-Bcl2 (SL-492, Santa Cruz Biotechnology, Santa Cruz, CA), normal rabbit IgG (Sigma, St. Louis, MO), anti-integrin $\alpha_5\beta_1$ (Protein G-purified from rabbit serum containing antibodies raised against human fibronectin receptor), and anti-metadherin(378-440). To detect bound antibodies, cells were incubated with goat anti-rabbit IgG-FITC (40 μg/ml in PBSB; Molecular Probes, Eugene, OR). After the final wash, the cells were resuspended with PBS containing 2 μg/ml of propidium iodide (PI) and analyzed by FACS.

HEK293T cell homing

HEK293T cells were cotransfected with DsRed2 (Clontech) and either metadherin-pCMV or empty myc-pCMV vector. 2 days posttransfection, the cells were detached with PBSE and filtered through a 40 μm nylon filter. DsRed2-expressing cells were isolated using a FACS Vantage flow cytometer (BD Biosciences, San Jose, CA). 2.5×10^5 DsRed2-positive cells were injected into the tail vein of nude Balb/c mice. Five mice were injected with each cell type. After 2 hr, the mice were sacrificed, organs were removed and fixed with 4% paraformaldehyde in PBS, and 10 μm thick frozen tissue sections were prepared. For each lung section, three different fields were counted. Clumps of DsRed2-positive cells with three or more cells were excluded from the count. Five sections per lung were counted.

Tumor metastasis studies

The 4T1 cells were detached from plates with PBSE, washed once with PBS, resuspended to 5×10^5 cells/ml in PBS, and placed on ice. Anti-

metadherin$_{(378-440)}$ or rabbit IgG (200 μg) was added to 5 × 10^4 cells and the cells were then injected via the lateral tail vein into female Balb/c nu/nu mice. Animals were sacrificed 7 days after tumor cell injection. Lungs were recovered and fixed with Bouin's solution, and the tumor foci on the surface of the left lobe were counted under a dissecting microscope.

siRNA knockdown of metadherin expression
For the siRNA-mediated knockdown of metadherin expression, nucleotides 1597–1615 of the mouse metadherin cDNA (5′-GTGCCACCGATGTTAC AAG-3′) were used as the target sequence. Oligonucleotides containing this target sequence were synthesized and subcloned into the pSilencer 3.0-H1 plasmid (Ambion, Austin, TX) according to the manufacturer's instructions. 4T1 cells were transfected with the metadherin or a negative control siRNA pSilencer vector together with an EGFP-expression vector (Clontech), using a 4:1 ratio of pSilencer to EGFP vectors. 2 days posttransfection, 4T1 cells that were labeled with EGFP and excluded propidium iodide were isolated by FACS. 10,000 or 50,000 of these selected 4T1 cells in 100 μl of PBS were injected into the tail vein of anesthetized nude Balb/c mice. The mouse lungs were harvested 22 days postinjection and fixed with Bouin's solution. The tumor foci on the lung surface were counted under a dissecting micro-scope. Data were recorded as the number of tumor foci formed per 10,000 cells injected. The levels of β-actin and metadherin mRNA in siRNA-trans-fected cells were determined using a one-step RT-PCR RNA Amplification Kit and LightCycler Instument (according to manufacturer's protocol; Roche, Indianapolis, IN).

GenBank accession number
The nucleotide sequence of the mouse metadherin cDNA has been depos-ited in GenBank and received accession number AY553638.

References

Abdel-Ghany, M., Cheng, H.C., Elble, R.C., and Pauli, B.U. (2001). The breast cancer beta 4 integrin and endothelial human CLCA2 mediate lung metastasis. J. Biol. Chem. *276*, 25438–25446.

Altschul, S.F., Madden, T.L., Schaffer, A.A., Zhang, J., Zhang, Z., Miller, W., and Lipman, D.J. (1997). Gapped BLAST and PSI-BLAST: a new generation of protein database search programs. Nucleic Acids Res. *25*, 3389–3402.

Amer, M.H. (1982). Chemotherapy and pattern of metastases in breast can-cer patients. J. Surg. Oncol. *19*, 101–105.

Arap, W., Pasqualini, R., and Ruoslahti, E. (1998). Cancer treatment by targeted drug delivery to tumor vasculature in a mouse model. Science *279*, 377–380.

Arap, W., Haedicke, W., Bernasconi, M., Kain, R., Rajotte, D., Krajewski, S., Ellerby, H.M., Bredesen, D.E., Pasqualini, R., and Ruoslahti, E. (2002). Targeting the prostate for destruction through a vascular address. Proc. Natl. Acad. Sci. USA *99*, 1527–1531.

Aslakson, C.J., and Miller, F.R. (1992). Selective events in the metastatic process defined by analysis of the sequential dissemination of subpopula-tions of a mouse mammary tumor. Cancer Res. *52*, 1399–1405.

Berlin, O., Samid, D., Donthineni-Rao, R., Akeson, W., Amiel, D., and Woods,

V.L., Jr. (1993). Development of a novel spontaneous metastasis model of human osteosarcoma transplanted orthotopically into bone of athymic mice. Cancer Res. *53*, 4890–4895.

Boogerd, W. (1996). Central nervous system metastasis in breast cancer. Radiother. Oncol. *40*, 5–22.

Chambers, A.F., Groom, A.C., and MacDonald, I.C. (2002). Dissemination and growth of cancer cells in metastatic sites. Nat. Rev. Cancer *2*, 563–572.

Cheng, H.C., Abdel-Ghany, M., Elble, R.C., and Pauli, B.U. (1998). Lung endothelial dipeptidyl peptidase IV promotes adhesion and metastasis of rat breast cancer cells via tumor cell surface-associated fibronectin. J. Biol. Chem. *273*, 24207–24215.

Dexter, D.L., Kowalski, H.M., Blazar, B.A., Fligiel, Z., Vogel, R., and Heppner, G.H. (1978). Heterogeneity of tumor cells from a single mouse mammary tumor. Cancer Res. *38*, 3174–3181.

Elble, R.C., Widom, J., Gruber, A.D., Abdel-Ghany, M., Levine, R., Goodwin, A., Cheng, H.C., and Pauli, B.U. (1997). Cloning and characterization of lung-endothelial cell adhesion molecule-1 suggest it is an endothelial chloride channel. J. Biol. Chem. *272*, 27853–27861.

Fidler, I.J. (2001). Seed and soil revisited: contribution of the organ microenvi-ronment to cancer metastasis. Surg. Oncol. Clin. N. Am. *10*, 257–269.

Glasgow, J. (1998). Proceedings, Sixth International Conference on Intelli-gent Systems for Molecular Biology: June 28–July 1, 1998, Montreal, Quebec (Menlo Park, CA: AAAI Press).

Harris, J., Morrow, M., and Norton, L. (1997). Malignant tumors of the breast. In Cancer: Principles and Practice of Oncology (Philadelphia: Lippincott-Raven), pp. 1557–1616.

Hoffman, J.A., Laakkonen, P., Porkka, K., Bernasconi, M., and Ruoslahti, E. (2004). *In vivo* and *ex vivo* selections using phage-displayed libraries. In Phage Display: A Practical Approach, T. Clackson and H. Lowman, eds. (Oxford, UK: Oxford University Press).

Johnson, R.C., Zhu, D., Augustin-Voss, H.G., and Pauli, B.U. (1993). Lung endothelial dipeptidyl peptidase IV is an adhesion molecule for lung-meta-static rat breast and prostate carcinoma cells. J. Cell Biol. *121*, 1423–1432.

Kamby, C., Dirksen, H., Vejborg, I., Daugaard, S., Guldhammer, B., Rossing, N., and Mouridsen, H.T. (1987). Incidence and methodologic aspects of the occurrence of liver metastases in recurrent breast cancer. Cancer *59*, 1524–1529.

Krogh, A., Larsson, B., von Heijne, G., and Sonnhammer, E.L. (2001). Pre-dicting transmembrane protein topology with a hidden Markov model: appli-cation to complete genomes. J. Mol. Biol. *305*, 567–580.

Kyte, J., and Doolittle, R.F. (1982). A simple method for displaying the hy-dropathic character of a protein. J. Mol. Biol. *157*, 105–132.

Laakkonen, P., Porkka, K., Hoffman, J.A., and Ruoslahti, E. (2002). A tumor-homing peptide with a targeting specificity related to lymphatic vessels. Nat. Med. *8*, 751–755.

Laemmli, U.K. (1970). Cleavage of structural proteins during the assembly of the head of bacteriophage T4. Nature *227*, 680–685.

Lal, A., Lash, A.E., Altschul, S.F., Velculescu, V., Zhang, L., McLendon, R.E., Marra, M.A., Prange, C., Morin, P.J., Polyak, K., et al. (1999). A public database for gene expression in human cancers. Cancer Res. *59*, 5403–5407.

Lash, A.E., Tolstoshev, C.M., Wagner, L., Schuler, G.D., Strausberg, R.L., Riggins, G.J., and Altschul, S.F. (2000). SAGEmap: a public gene expression resource. Genome Res. *10*, 1051–1060.

Luo, L., Salunga, R.C., Guo, H., Bittner, A., Joy, K.C., Galindo, J.E., Xiao, H., Rogers, K.E., Wan, J.S., Jackson, M.R., and Erlander, M.G. (1999). Gene expression profiles of laser-captured adjacent neuronal subtypes. Nat. Med. *5*, 117–122.

McIntosh, D.P., Tan, X.Y., Oh, P., and Schnitzer, J.E. (2002). Targeting endothelium and its dynamic caveolae for tissue-specific transcytosis in vivo: a pathway to overcome cell barriers to drug and gene delivery. Proc. Natl. Acad. Sci. USA *99*, 1996–2001.

Mechler, B.M. (1987). Isolation of messenger RNA from membrane-bound polysomes. Methods Enzymol. *152*, 241–248.

Miller, F.R., Miller, B.E., and Heppner, G.H. (1983). Characterization of metastatic heterogeneity among subpopulations of a single mouse mammary tumor: heterogeneity in phenotypic stability. Invasion Metastasis *3*, 22–31.

Muller, A., Homey, B., Soto, H., Ge, N., Catron, D., Buchanan, M.E., McClanahan, T., Murphy, E., Yuan, W., Wagner, S.N., et al. (2001). Involvement of chemokine receptors in breast cancer metastasis. Nature *410*, 50–56.

Orr, F.W., and Wang, H.H. (2001). Tumor cell interactions with the microvasculature: a rate-limiting step in metastasis. Surg. Oncol. Clin. N. Am. *10*, 357–381.

Pasqualini, R., and Ruoslahti, E. (1996). Organ targeting in vivo using phage display peptide libraries. Nature *380*, 364–366.

Porkka, K., Laakkonen, P., Hoffman, J.A., Bernasconi, M., and Ruoslahti, E. (2002). A fragment of the HMGN2 protein homes to the nuclei of tumor cells and tumor endothelial cells in vivo. Proc. Natl. Acad. Sci. USA *99*, 7444–7449.

Price, J.E., Polyzos, A., Zhang, R.D., and Daniels, L.M. (1990). Tumorigenicity and metastasis of human breast carcinoma cell lines in nude mice. Cancer Res. *50*, 717–721.

Pulaski, B.A., and Ostrand-Rosenberg, S. (1998). Reduction of established spontaneous mammary carcinoma metastases following immunotherapy with major histocompatibility complex class II and B7.1 cell-based tumor vaccines. Cancer Res. *58*, 1486–1493.

Radinsky, R. (1995). Modulation of tumor cell gene expression and phenotype by the organ-specific metastatic environment. Cancer Metastasis Rev. *14*, 323–338.

Rajotte, D., and Ruoslahti, E. (1999). Membrane dipeptidase is the receptor for a lung-targeting peptide identified by in vivo phage display. J. Biol. Chem. *274*, 11593–11598.

Rajotte, D., Arap, W., Hagedorn, M., Koivunen, E., Pasqualini, R., and Ruoslahti, E. (1998). Molecular heterogeneity of the vascular endothelium revealed by in vivo phage display. J. Clin. Invest. *102*, 430–437.

Ruoslahti, E. (2002). Specialization of tumour vasculature. Nat. Rev. Cancer *2*, 83–90.

Rutgers, E.J., van Slooten, E.A., and Kluck, H.M. (1989). Follow-up after treatment of primary breast cancer. Br. J. Surg. *76*, 187–190.

Tomin, R., and Donegan, W.L. (1987). Screening for recurrent breast cancer—its effectiveness and prognostic value. J. Clin. Oncol. *5*, 62–67.

van 't Veer, L.J., Dai, H., van de Vijver, M.J., He, Y.D., Hart, A.A., Mao, M., Peterse, H.L., van der Kooy, K., Marton, M.J., Witteveen, A.T., et al. (2002). Gene expression profiling predicts clinical outcome of breast cancer. Nature *415*, 530–536.

Weiss, L. (1992). Comments on hematogenous metastatic patterns in humans as revealed by autopsy. Clin. Exp. Metastasis *10*, 191–199.